Pilot-scale study of sorption-enhanced gasification of sewage sludge

Samuel Moles[1], Isabel Martinez[2*], María Soledad Callén[2], Jairo Gómez[3], José Manuel López[2], Ramón Murillo[2]

[1] Environmental Sciences Research Institue (IUCA). University of Zaragoza. c. Pedro Cerbuna, 12, 50009 Zaragoza (Spain)

[2]Environmental Research Group, Instituto de Carboquímica (Spanish National Research Council, ICB-CSIC), Miguel Luesma Castán 4, 50018 Zaragoza (Spain)

[3]Navarra de Infraestucturas Locales S.A. Av. de Barañáin, 22, 31008 Pamplona (Spain)

*corresponding author: imartinez@icb.csic.es

Abstract

Sustainable management and disposal alternatives for sewage sludge (SS) should be pursued due to the substantial increment in its global production, as well as due to the raising interest in the renewable energy and synthetic fuels deployment. Since SS present high moisture (> 95% wt.) drying would play an essential role in SS management. In this work, SS pre-treated in a solar-drying facility has been successfully used as feedstock in a 30 kW_{th} bubbling fluidised-bed (BFB) gasification pilot plant operating under Sorption Enhanced Gasification (SEG) conditions, i.e. using CaO as bed material and steam as gasifying agent. The influence of key operating SEG parameters (such as temperature, steam-to-carbon ratio and sorbent-to biomass proportion) in the syngas yield and composition (H_2, CO, CO_2, CH_4, C_xH_y, H_2S, COS, NH_3 and tars) has been carefully assessed. As a matter of comparison, steam-oxygen gasification conditions have been also tested in the facility using solar-dried SS as feedstock. The results obtained demonstrate the possibility of producing a syngas with high H_2 contents of 70-73 vol.% and relatively low CO and CO_2 contents (i.e. 2-3 vol.% and 8 vol.% respectively).

Keywords: sewage sludge, sorption enhanced gasification, tailored syngas

1. **Introduction**

Water treatments employed are capable of reducing the concentration of hazardous compounds in wastewater [1–5], resulting in the production of sewage sludge (SS) as a by-product. The generation of sewage sludge in Europe (EU27) is estimated to be around 10 million tonnes (in terms of dry solids) [6]. Despite the vast quantities of SS produced globally, its properties and potential uses remain underexplored. In the year 2021, nearly half (48 %) of this was utilized for land applications in agriculture, while about 27% was subjected to incineration. Landfilling has significantly decreased due to governmental regulations (6 %) [7]. Sewage sludge management practices vary widely across the member nations. For instance, while nutrient recycling in agriculture (either through direct land spreading or composting) is the predominant practice in countries like Spain, Ireland, Finland, and Hungary, the main avenue for SS application has been agriculture, with about 80 % of SS in Spain presently used in this sector, according to the National Registry of Sludge data [8]. This metric underscores the urgent need for highly effective and ecologically sustainable strategies for SS management. Furthermore, it emphasizes the importance of innovation and collaboration across sectors to develop and implement solutions that not only solve the SS management problem, but also contribute positively to the environment and society, such as biofuels production.

SS is a complex matrix that contains contaminants of emerging concern (CECs), such as microplastics or pharmaceuticals, as well as pathogens or heavy metals [9,10]. Despite heavy metals being controlled, the direct introduction of uncontrolled substances such CECs into the soil could pose serious environmental risks. In addition, its high water content leads to further difficulties for SS management, such as transport. Solar drying is a promising low-cost alternative for removing moisture, as it utilizes free solar energy

to reduce operational costs and the overall pathogen content in the SS, while also reducing the overall quantity of SS [11]. In this context, it is imperative to explore and develop environmentally-conscious approaches for the valorisation of SS. For instance, biofuels production from SS can help not only in reducing greenhouse gas emissions, but also in protecting the environment, minimizing the volume of SS, and avoiding soil pollution [12].

Directive 2018/851/EC in Europe established a waste prevention hierarchy in which material recovery and energy recovery are the most recommended methods for managing SS [13]. In this framework, several SS valorisation options for material recovery have been investigated recently. For example, due to its high phosphorus and nitrogen content, SS can be utilized to produce fertilizers such as struvite, allowing for the easy commercialization of recycled phosphorus [14]. Additionally, SS valorisation through construction materials has been widely documented [15–17]. Moreover, thermochemical processes offer an interesting approach to SS disposal while simultaneously generating renewable energy. Incineration is the conventional thermochemical process for SS. Around 8 % of the total SS volume in Spain is incinerated, according to the Spanish Government [8]. Syed-Hassan et al. (2017) reviewed the state of the art of thermochemical processes applied to SS, outlining the challenges, fundamentals, and considerations for SS incineration [18]. Among these challenges, the emission of air pollutants is a significant obstacle for this valorisation route. Recently, Yu Liang et al. (2021) reviewed the literature related to pollutant emission reduction from SS incineration in recent years, summarizing the formation and transformation mechanisms of pollutants (e.g., heavy metals, nitrogen and sulphur oxides) [19]. Their findings suggested that air pollution remains a significant challenge for SS incineration.

Moreover, existing literature suggests that gasification of SS could provide an environmentally sustainable means of energy production [20]. This process significantly reduces pollutant air emissions in comparison with incineration, and results in the production of syngas as the primary output. This versatile precursor offers a valuable solution for addressing environmental pollution and the energy crisis, as it can be used for alternative fuel, chemical and electricity production [21]. Additionally, gasification of SS allows the complete destruction of pathogenic microorganisms and a significant volume reduction of SS [18]. However, one of the primary barriers to the use of SS gasification is the high moisture content of raw SS material, which typically exceeds 90%. Therefore, it is necessary to dry the SS prior to feeding it into the gasification system [21]. This requirement represents a significant obstacle in the application of thermochemical processes, according to the literature [16,22]. A trendy low-cost alternative to remove the SS moisture is solar drying [11].

One of the most cost-effective thermochemical conversion routes for the conversion of residues into synthetic fuels is the sorption-enhanced gasification (SEG) process. This process is a promising technology for the gasification of several feedstocks, including biomass, coal, SS or municipal solid waste. The SEG process involves the use of a Ca-based sorbent material that reacts with the CO_2 produced during gasification, pushing the reactions towards the production of H_2. Moreover, the carbonation of CaO provides part of the energy needed for the endothermic gasification reactions together with the sensible heat of the hot CaO that is fed into the gasifier coming from a secondary combustion reactor. In fact, the $CaCO_3$ formed is regenerated in this secondary reactor or combustor at high temperature, releasing the captured CO_2 and allowing the sorbent to be reused in subsequent cycles. Furthermore, one of the most important features of this SEG process is the possibility of acting on SEG parameters (i.e. temperature and

105 sorbent/biomass proportion) to obtain a syngas with a correct ratio of H_2, CO and CO_2
106 based on the desired final product application, which would simplify noticeably the
107 conditioning reactors placed downstream [21]. This SEG process has already been
108 demonstrated in various laboratory and pilot-scale facilities throughout Europe [23],
109 under conditions that are suitable for achieving elevated H_2 concentrations in the
110 syngas.

111 Steam-oxygen gasification has been also proposed in the literature for obtaining a
112 syngas with relevant mole fractions of H_2 and CO as to make it suitable for the
113 synthesis of transport fuels or chemicals. In this gasification mode, oxygen is used for
114 providing the necessary heat for the endothermic gasification reactions through partial
115 oxidation of the produced syngas. Several research works have studied the use of highly
116 volatile feedstocks, such as SS, in dual fluidized bed pilot systems using CaO or inert
117 bed material under steam/O_2 gasification conditions [24–26]. Such works have
118 demonstrated that the addition of CaO can be a low cost measure for reducing tar and
119 sulfur cleaning efforts, whereas it has not effect on ammonia emissions [26]. The use of
120 limestone as bed material increases the ash melting point, decreasing the risk of bed
121 agglomeration. The literature founds that the impurity concentrations in sewage sludge-
122 derived product gas are higher than in straw-derived gas, particularly NH_3, which could
123 be recovered as a valuable product [26].

124 In this context, the main goal of this study is to validate the use of solar dried SS as
125 feedstock material for the production of tailored syngas by means of a SEG process in a
126 30 kW_{th} bubbling fluidised-bed (BFB) gasification pilot plant. Steam-oxygen
127 gasification conditions have been already explored in the published literature for SS as
128 feedstock using CaO as bed material [22,24,26] as well as steam gasification with the
129 addition of CaO into a bed material consisting of silica sand [25]. However, to the

author's knowledge, it is the first time in the literature that SEG conditions (i.e. steam as gasifying agent and CaO as bed material) have been tested at relevant scale for solar dried SS as fuel. Syngas yield and composition as well as impurities formation (i.e. tar, H_2S, COS and NH_3) have been carefully analysed for different operating conditions. For the sake of a rigorous comparison in terms of syngas quality, conventional steam-oxygen gasification conditions were also studied in the gasification facility using the same solar dried SS as feedstock.

2. **Materials and methods**

2.1. Feedstocks

2.1.1. Sewage sludge

The SS was produced in an urban wastewater treatment plant in the Ebro Basin, Spain. The ultimate and proximate analyses of SS were determined, after stabilising SS samples in a climatic chamber Memmert ICH110eco until equilibrium moisture content was reached, obtaining the results compiled in Table 1. Ultimate analysis (carbon, hydrogen, nitrogen and sulphur) was determined in a LECO 628 Serie equipment (UNE-EN 150407:2011) where complete combustion of the sample occurs inside a high-temperature reactor followed by an accurate chromatographic analysis of the flue gas. Moisture, volatile matter and ash contents were calculated according to UNE-EN 15414-3:2011, UNE-EN 15402:2011 and UNE-EN 15403:2011 standards, respectively. The determination of calorific value was not possible due to the presence of Al in the sample. Ash composition was also measured by inductively coupled plasma-optical emission spectrometry (ICP-OES), obtaining the results shown in Table 2. To determine ash composition, sample was calcined in a muffle oven at 550 ºC for obtaining the ashes. It was then crushed and homogenised before being digested with lithium

tetraborate. Chemical composition has been expressed as the percentage of metal in the ashes, but it should be noticed that these metals would be in their oxide form (i.e. Al_2O_3, CaO, Fe_2O_3, etc..). Thus, the remaining percentage up to 100% will be mostly oxygen.

Table 1. Ultimate and proximate analysis of SS used as feedstock

Ultimate analysis [wt. %]		**Proximate analysis**	**[wt.%]**
C	32.60	Volatile Mater	52.30
H*	4.68	Ash	25.60
N	5.22	Moisture	11.80
S	0.97	Fixed Carbon	10.30
O*	19.13		

*The H content excludes the H content in the moisture

**The O content has been calculated as 100-C-H-N-S-Ash-Moisture

Table 2. Ash chemical composition (expressed as weight percentage in the ashes) of the SS used as feedstock in this work

	wt% in the ashes
Al	3.4
Ca	15.0
P	10.9
Fe	5.5
Mg	2.6
Mn	<0.025%
K	2.3
Si	9.2
Na	0.3
Ti	0.4

Solar radiation allows for significant reduction of moisture content by utilizing free and renewable energy. The SS is spread in layers in the floor of the solar drier shown in Figure 1. This chamber has a fan to achieve the correct air ventilation to renew saturated humid air by fresh air. In addition, the solar drier is provided with a stirring robot to mix the product several times in a day to obtain a homogeneous product and deal with the

common heterogeneity of SS. The raw SS contained more than 90 wt.% of moisture. Feeding the gasifier with raw SS containing such high moisture content would be impractical for several reasons: (i) the water in the SS should be evaporated within the gasifier, which implies a significant energy consumption that penalises the energy conversion efficiency of the process [27]; (ii) in the pilot facility in this work, SS was fed by a screw feeder that will not be able to work properly with raw SS. For these reasons, the sludge was first dewatered up to 80 wt.% of moisture by centrifugation, before being dried in the solar drier until reaching ideal moisture percentage, which according to the literature should be between 10-15 wt.%. Taking into account that the average specific energy consumption for SS drying could represent up to 2.7 kWh/kg using conventional drying processes (i.e. air driers), solar drying would allow reducing significantly such specific energy consumption below 1.9 kWh/kg [28]. After the drying process, SS was sieved to achieve a particle size lower than 18 mm to facilitate its feeding to the gasification pilot plant. Finally, the average particle size was 10 mm.

Figure 1. (left) Pilot-scale solar drier of SS outside photo (right) Pilot-scale solar drier of SS inside photo

2.1.2. Bed materials

SEG experiments were performed using calcined limestone as bed material in the reactor, which was supplied by LHOIST Germany/Rheinkalk GmbH. This material was

obtained by calcining limestone in the BFB pilot plant at ca. 900 ºC by means of the combustion of a high-grade fuel containing <0.02 wt% of sulphur. Table 3 shows the chemical composition of the calcined limestone determined by ICP-OES and expressed as the most probable metal oxide form. As appreciated in this table, this calcined material has a CaO content of ca. 90 wt% with MgO, Fe_2O_3 and SiO_2 as main impurities. Particle size of the calcined sorbent used for the SEG tests was 100-300 μm. Steam-oxygen gasification experiment was performed using magnesite as bed material, which was supplied by Magnesitas de Navarra S.A. The chemical composition of this material was also determined through ICP-OES, obtaining the results indicated in Table 3. This mineral consisted mainly of MgO (76.5 wt.%) with CaO, Fe_2O_3, SiO_2 and Al_2O_3 as main impurities. Particle size of the magnesite material used for the steam-oxygen gasification test was 200-500 μm.

Table 3. Composition of the calcined limestone and magnesite used in SEG and steam-oxygen experiments, respectively

	Calcined limestone (% wt)	**Magnesite (% wt)**
CaO	89.55	6.23
Fe_2O_3	0.10	3.02
MgO	1.16	76.52
SiO_2	0.24	4.39
Al_2O_3	--	1.35
K_2O	--	0.14
MnO_2	--	0.28
$CaSO_4$	--	0.13

2.2. 30 kW_{th} gasification pilot plant

Gasification tests in this work were performed in a 30 kW_{th} gasification plant located at ICB-CSIC, referred to the nominal thermal input. Considering an average low heating

209 value of SS of 15-21 MJ/kg [29–31]and 2 kg/h of SS the thermal input in the range 8.3-
210 11.7 kWth. The flowsheet of this pilot plant is shown in Figure 2. This facility consists
211 of a bubbling fluidized bed (BFB) reactor standing 3 m in height and comprising a
212 dense bottom zone with an internal diameter of 0.15 m. A lateral overflow regulates
213 solid bed inventory in the bottom zone of the reactor and allows pulling out from the
214 reactor partially converted solids that are collected in a hopper that is periodically
215 discharged during the operation. SS and bed material (calcined limestone or magnesite)
216 are fed separately into the reactor by means of two independent screw feeders (see
217 Figure 2**¡Error! No se encuentra el origen de la referencia.**). The reactor is externally
218 heated through different electrical resistance elements and insulated with glass wool.
219 There are seven thermocouples and four pressure transducers throughout the height of
220 the reactor vessel as indicated in the figure. Two high efficiency cyclones separate
221 entrained solids (i.e. bed material particles and unconverted char) generated during the
222 gasification process. The syngas is then cooled in a shell-and-tube condenser using tap
223 water as coolant, and then passes through a commercial filter before being burnt in a
224 flare to be emitted to the atmosphere. Specific details of this pilot plant have been
225 already given in previous publications [32–34]

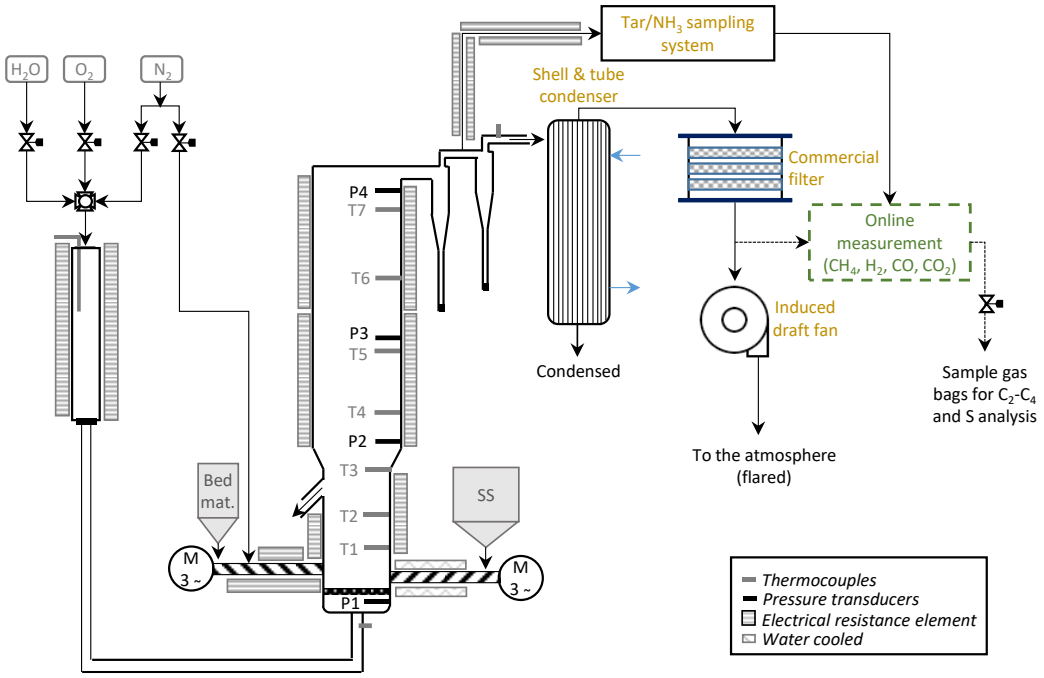

Figure 2. Scheme of the 30 kW_{th} BFB gasification pilot plant

Permanent gas content in the syngas produced (i.e. H_2, CH_4, CO and CO_2) is measured online using a SICK GMS810 analyzer that is placed downstream the filter or downstream the tar/NH_3 sampling system, as indicated in Figure 2. In addition, tedlar sampling bags are taken during steady-state operation for off-line gas analysis by gas chromatography to determine the content of permanent gases and light hydrocarbons (up to C_4). Permanent gases were analysed in a Bruker 450 gas chromatograph (GC) equipped with a thermal conductivity detector (TCD). Separation was performed by using two stainless steel packed columns in series (Molsieve 13X and HayeSep Q). An oven temperature of 60 ºC was maintained for 8 min. The carrier gas was Argon at a constant column flow rate of 30 Nml/min. The TCD temperature was 200 ºC. Certified gas mixtures (Air Products) were used for identification and quantification purposes. The light hydrocarbons (methane, ethane, ethylene, propane, propylene, isobutane, n-butane, trans-2-butene, 1-butene, isobutene, cis-2-butene and 1,3-butadiene) were analysed in a PerkinElmer Clarus 590 gas GC equipped with a flame ionisation detector

(FID). Separation was performed by a 30-m-long and 0.32-mm-wide alumina chloride capillary column. An initial oven temperature of 40 ºC was maintained for 2.5 min, after which a heating rate of 5 ºC/min was implemented to reach an oven temperature of 90 ºC. The heating rate was then increased to 15 ºC/min to reach the final oven temperature of 180 ºC. This temperature was maintained for 4.5 min. The carrier gas was Helium with an initial pressure of 9 psi for 16 min, and then rose to 18 psi. The injector and FID temperatures were both 250 ºC. Certified gas mixtures (Air Products) were used for identification and quantification purposes.

Table 4 summarizes the gasification experiments performed in this work using SS as feedstock. The experimental routine followed in the experiments has been already explained in a previous work [32]. During steady-state operation, which was kept for ca. 1h, gas and solid samples were taken every 10/15 min from the overflow, cyclones and the gas line connected to the analyzer, whereas tar and NH_3 samples were taken in parallel as explained in section 2.3.1. Variables studied in SEG experiments were the gasification temperature, the steam-to-carbon (S/C) ratio (defined as the moles of steam introduced into the gasifier per mole of C introduced with the SS) and the sorbent-to-biomass (Sr/B) ratio (weight basis). The Ca/C ratio is defined as the moles of Ca introduced with the sorbent per mole of C introduced with the SS, and it is calculated from the Sr/B ratio but accounting for the Ca purity of the calcined limestone. As noticed in the table, SEG.1 and SEG. 2 experiments were performed under the same conditions of S/C and Sr/B (and so Ca/C) proportions but at different temperatures, whereas SEG.2 and SEG.3 experiments correspond to the same operating temperature but different S/C and Sr/B proportions. Concerning the steam-oxygen gasification experiment (referred to as S-O2 in Table 4), it was performed keeping the same mass flow rate of SS that in SEG experiments but introducing a mixture of steam and O_2 as

gasifying agent. The amount of O_2 introduced in this case is given by the equivalence ratio (ER) that is defined as the moles of O_2 introduced into the gasifier per mole of stoichiometric O_2 needed for the complete combustion of the SS introduced into the reactor. The stoichiometric amount of O_2 was calculated using the ultimate analysis of the SS indicated in Table 1. In this case, the parameters ER and S/C were aimed at values close to 0.2 and 1 respectively, since these were the commonly used parameters in steam-oxygen gasification [24,26,35]. The operating temperature indicated in Table 4 corresponds to the average temperature reached during the steady-state period in the bottom dense zone of the reactor in each experiment (corresponding to the average value of T1 and T2 in Figure 2). The temperature profile in the reactor (corresponding to temperature T3, T4, T5, T6 and T7) was kept similar to the temperature in the bottom dense zone of the reactor in every experiment by means of the electrical resistance elements placed throughout the reactor height. Figure 3 shows the temperature profiles along the reactor height during steady-state period for tests SEG.3 and S-O2. As appreciated, solid bed temperature remained quite stable during the steady-state period with variations of < 2ºC due to the vigorous fluidization conditions used for these experiments. More precisely, $u_0/u_{mf} > 4$ for all the conducted experiments, which has reported in previous work at pilot scale facilities [33,36] According to the literature, applying these fluidization conditions, it has been observed a reduction of unconverted char segregation [37]. Freeboard temperatures were kept similar to those of the solid bed by means of the electrical resistance elements placed along the reactor, keeping the variations in the average temperature below 20 ºC. The final part of the reactor remained cold at ca. 400ºC due to the heat losses at this location.

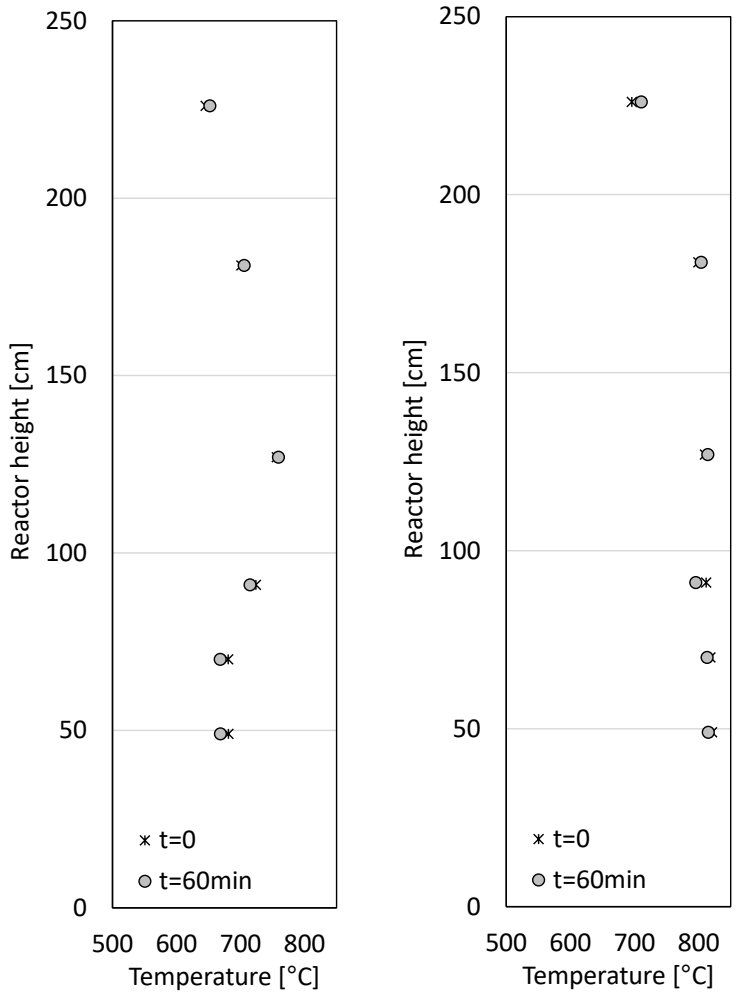

Figure 3. Temperature profiles along the reactor during SEG.3 (right) and S-O2 (left) experiments in Table 4

Table 4. Operating conditions used for the experiments performed in this work.

No.	Gasifying agent	SS feeding rates [kg/h]	Bed material feeding rates [kg/h]	S/C ratio [mol/mol]	ER [mol/mol]	Sr/B ratio [kg/kg]	Ca/C ratio [mol/mol]	Temperature [ºC]
SEG.1	Steam	1.8	4.1	1.0	--	2.2	1.0	640
SEG.2	Steam	1.6	3.9	1.1	--	2.4	1.0	685
SEG.3	Steam	1.1	4.0	1.8	--	3.7	1.5	680
S-O2	Steam/O_2	1.5	3.4	1.1	0.2	2.2	--	815

**In the S-O2 test, magnesite (MgO) was used as bed material. Overflow solids consisted mainly of MgO with minor quantities of $CaCO_3$ due to the small quantity of CaO in the magnesite*

2.3. Products characterization

2.3.1. Syngas impurities

An offline method for tar sampling was used based on the Neeft protocol for biomass gasification [38]. The method involved passing the syngas through a train of seven impinger bottles, five of which contained 100 ml of isopropanol, while the first and seventh bottle were left empty. The impingers were positioned in two cooling baths, with four impingers (1, 2, 3, and 5) at room temperature and three (4, 6, and 7) at −20 °C. A slipstream of hot syngas was extracted between the first and second cyclone for tar sampling, with its flow rate controlled by a pump. This slipstream was then directed through a metallic filter and a heated line (both at 400 °C) directly into the impinger system. Tar sampling was performed for a period of 30 minutes for all experiments, and the sampled gas volume varied between 0.05 and 0.15 Nm^3 of dry gas. Two different methods were used for the quantification of tar: namely gravimetric tar and GC-MS tar.

The quantitative determination of the compounds in the isopropanol solution was performed using a Perkin-Elmer Clarus 690 gas chromatograph coupled to a Clarus SQ8 quadrupole mass spectrometer (GS-MS). The system was equipped with a capillary column, Elite-5ms (5% diphenyl-95% dimethylpolysiloxane; 60 mx0.25 mm, 0.250 μm). For the analysis, an initial oven temperature of 60 °C was maintained for 3 minutes, followed by a sustained heating rate of 7 °C/min until a final temperature of 300 °C was reached for about 16 minutes. The carrier gas used was He (BIP quality) at a constant column flow rate of 1 ml/min. The injector, source, and transfer line temperatures were set at 300 °C, 250 °C, and 260 °C, respectively. 1 microliter of sample was automatically injected with an auto-sampler with a split flow of 20 ml/min. Over 23 compounds were identified and quantified by external calibration using both,

322 the full scan and the selected ion recording (SIR) mode with specific ions as the
323 quantification ion, and the full list is presented in Table 5. Each tar sample was
324 quantified in duplicate by GC-MS, and the relative standard deviation (RSD) was below
325 15%.

326 **Table 5. List of compounds identified and quantified in GC-MS**

Tar classification group	GCMS compounds
BTX	Benzene, toluene, ethylbenzene, (p+m)xylene, o-xylene
PAHs	Naphthalene, acenaphthylene, acenaphthene, fluorene, phenanthrene, anthracene, fluoranthene, pyrene, benzo(a)anthracene, chrysene, benzo(b)fluoranthene, benzo(a)pyrene, indeno (1,2,3-cd)pyrene, dibenz(a,h)anthracene, benzo(ghi)perylene
Phenols	Phenol, 4-methylphenol

327 Gravimetric tar was also determined for each experiment. An aliquot of 100 ml of the
328 collected tar solution was concentrated in a rotary evaporator until dryness, under
329 controlled temperature and vacuum conditions. The solid residue obtained was then
330 weighted in a microbalance with a precision of 0.1 mg, after being kept in a desiccator
331 for at least 12 hours. The solid residue was weighed three times until a constant weight
332 value was obtained. The gravimetric tar was calculated as the average weight value of
333 the solid residue in proportion to the dry gas volume that passed through the sampling
334 system during the analysis, and was expressed as g/Nm^3 dry gas. The maximum relative
335 standard deviation of 1.5% was determined for gravimetric tar, considering the different
336 weight values measured for each determination.

337 Sulphur compounds in the syngas were analysed in the tedlar sampling bags taken when
338 passing the syngas through the tar sampling system. A Perkin Elmer Clarus 590 gas
339 chromatograph equipped with a flame photometric detector (FPD) was used in this case

for sulphur compounds determination. The separation was performed using a 30 m Rt-Silica BOND capillary column, using an initial oven temperature of 45 °C that was maintained for 4 min, followed by a heating rate of 15 °C/min until reaching a final temperature of 200 °C, which was maintained for 2 min. The carrier gas used was N_2 at a constant column flow of 2 Nml/min. The injector and FPD temperatures were 250 °C and 300 °C, respectively. The sulphur compounds analysed included carbonyl sulphide (COS), hydrogen sulphide (H_2S), carbon disulphide (CS_2) and methyl mercaptan (CH_4S). Certificated gas mixtures from Air Products were used for identification and quantification purposes.

Finally, ammonia content in the syngas was determined according to the methodology proposed by the US Environmental Protection Agency [39]. Sample collection was performed by making the syngas pass through a series of five impingers placed in an ice bath that kept their temperature at 0 ºC. The scheme of the sampling set is shown in Figure 4. As shown in the figure, the first and last impingers were left empty, while the remaining three were filled with 100 mL of 0.1 N H_2SO_4. The solution containing ammonia in the form of NH_4^+ was then analysed in a Metrohm ion chromatograph with a conductivity detector (UNE-EN 15289) and an anionic column (model Metrosep C6).

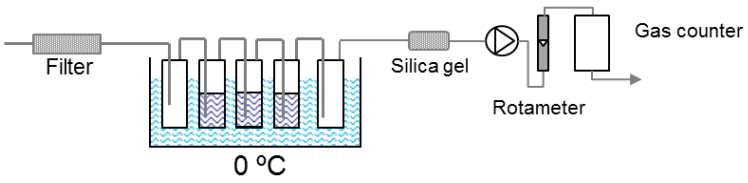

Figure 4. Scheme of the off-line NH_3 sampling method used

2.3.2. Solid samples

Solid samples were taken every 10/15 minutes over the steady-state period from the solids collected through the overflow and the entrained material separated in the cyclones. Solids collected through the overflow consisted of a mixture of coarse particles (>1 mm) that corresponded to unconverted SS pellets and smaller particles (<1 mm) that corresponded to partially carbonated bed material (for the case of SEG experiments) with small quantities of unconverted char. These overflow solids were sieved to separate coarse particles from small particles to be conveniently analyzed. Elutriated solids collected in the cyclones consisted mainly of carbonated bed material lost by attrition together with SS ashes.

Coarse particles collected through the overflow were analyzed to determine their ultimate and proximate analyses similarly to the procedures already described for the SS in section 2.1.1. This information was used for calculating a global fixed carbon conversion in each experiment as described previously in [33]. Smaller particles collected through the overflow as well as solids collected in the cyclones were analyzed through X-ray diffraction (XRD) to determine the nature of the crystalline phases and their relative amount. This technique was useful for detecting, for example, the presence of CaS in the solids separated in the cyclones. Moreover, smaller particles collected from the overflow were analyzed through thermogravimetric analysis (TGA) to determine the content of $CaCO_3$ (in the case of SEG experiments) and the content of unconverted char. The experimental procedure followed consisted of an initial heating period in N_2 until 850 ºC, followed by a period at 850 ºC in which air was used as carrier gas. During the first period in N_2, it was appreciated a main weight loss when reaching temperatures close to 700 ºC, which corresponded to the calcination of $CaCO_3$ into CaO. Then, when air was introduced into the TGA apparatus, another weight loss was observed that corresponds to the combustion of the unconverted char. From this

386 analysis, the fixed carbon content and the $CaCO_3$ content of the particles were
387 determined, which was used for the calculation of the global fixed carbon conversion.

388 3. **Results and discussion**

389 *3.1. Product gas yield and composition*

390 The effect of solid bed temperature, steam-to-carbon (S/C) ratio, sorbent-to-biomass
391 (Sr/B) ratio, and gasification mode on the product gas yield and composition was
392 analyzed first. Figure 5 shows the product gas yield (in Nm^3 gas (dry N_2-free) per kg of
393 sewage sludge fed into the gasifier), fixed carbon conversion and product gas
394 composition for the gasification experiments summarized in Table 4. Product gas
395 composition is given in volume fractions on a dry N_2-free basis. The effect of the solid
396 bed temperature, the S/C and the Sr/B ratios can be appreciated mainly in the gas yield
397 and fixed carbon conversion in the experiments performed under SEG conditions (three
398 left columns in Figure 5 top). As appreciated in the figure, total gas yield increased from
399 0.32 to 0.49 Nm^3 (dry N_2-free)/kg when gasification temperature moved from 640 ºC to
400 685 ºC, respectively (i.e. experiments SEG.1 and SEG.2). This increase in the product
401 gas yield with the gasification temperature is due to the enhancement of the primary
402 pyrolysis, steam cracking and reforming reactions, as well as char gasification [40,41].
403 Light hydrocarbons content in the product gas (i.e. CH_4, C_2H_4, C_2H_6, C_3H_6, C_3H_8 and
404 $>C_3$) barely changed with the gasification temperature as can be observed in Figure 5
405 down when comparing experiments SEG.1 and SEG.2, indicating that product gas yield
406 rise may be related to fixed carbon conversion variations in this case. In fact, calculated
407 fixed carbon conversion increased from ca. 30% to 56% when raising the temperature
408 from 640 ºC to 685 ºC, respectively as indicated in Figure 5 top.

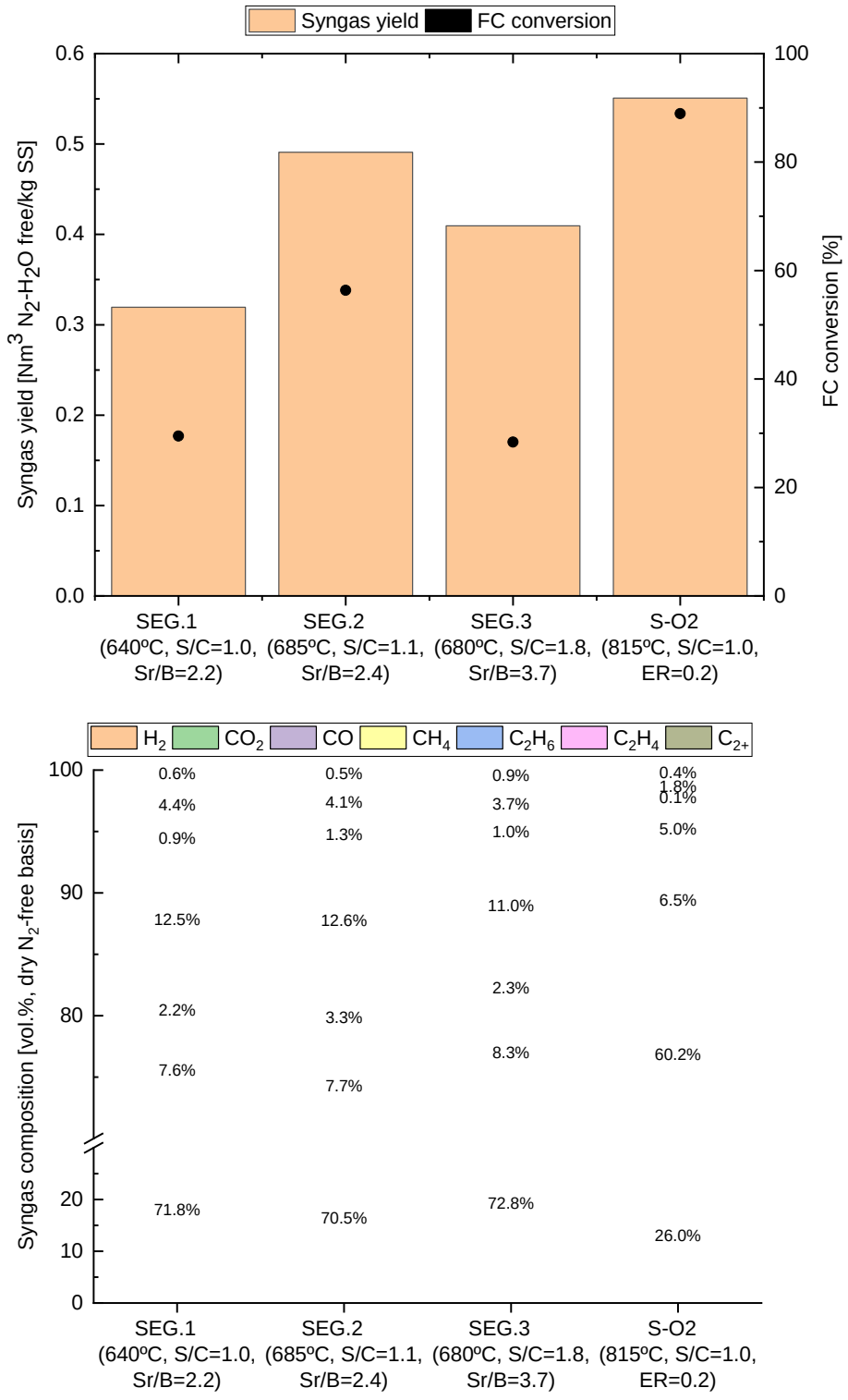

Figure 5. (top) total gas yield and fixed carbon conversion, and (down) product gas composition for the different experiments indicated in Table 4

The effect of increasing both the S/C and the Sr/B ratios under SEG conditions can be analysed comparing results from SEG.2 and SEG.3 experiments in Figure 5, which

were performed under the same temperature but raising S/C and Sr/B proportions in SEG.3 test (see Table 4 for detailed information on these experiments). Regarding the gas yield, it can be appreciated a decrease from 0.49 Nm^3 (dry N_2-free)/kg in experiment SEG.2 to 0.41 Nm^3 (dry N_2-free)/kg in experiment SEG.3. There are several facts influencing the observed impact on the total gas yield. On the one hand, the fixed carbon conversion decreased to ca. 28 % in experiment SEG.3 due to the lower residence time of the particles in the gasifier in this case. On the other hand, the amount of CO_2 separated in experiment SEG.3 was larger than in SEG.2 due to the larger Sr/B ratio (and so larger Ca/C ratio) . $CaCO_3$ content in the overflow solids, which was determined through TGA analysis according to the experimental procedure explained in section 2.3.2, was included in Table 4. Based on this information, the percentage of CO_2 separated in the gasifier was calculated as the moles of CO_2 collected as $CaCO_3$ in the overflow solids per mole of C introduced with the biomass during the same period of time. It was demonstrated that the percentage of CO_2 separated as $CaCO_3$ in SEG.3 experiment was of ca. 40 %, which was significantly larger than that separated in SEG.2 test that resulted in 28 %, confirming the aforementioned effect on the gas yield. Regarding syngas composition (Figure 5 down), it may be noticed that working under higher S/C and Sr/B ratios makes the syngas product to be enriched in H_2 and become poorer in CH_4 and CO since the enhancement of the carbonation reaction pushes the reforming of the hydrocarbons as well as the water gas shift reactions towards H_2 production. As appreciated in the figure, H_2 content increases up to 73.1 % (dry N_2-free basis) in experiment SEG.3, whereas CH_4 and CO contents decrease to 11 % and 2.3 % respectively.

Finally, the influence of the gasification mode used on the product gas yield and composition is discussed. In addition to the SEG experiments previously described,

steam-oxygen gasification conditions were also tested in the pilot plant using SS as feedstock. Operating conditions used in this experiment have been already indicated in Table 4, which has been referred to as "S-O2". Gasification temperature was kept at 815 ºC using an ER of 0.2 and an S/C ratio of 1.1. Magnesite was used as bed material in this case. Such operating conditions were chosen as reasonable for steam-oxygen gasification based on the conditions typically found in the literature for this gasification mode [24,26,35]. Gas yield, fixed carbon conversion and syngas composition obtained under steam-oxygen gasification conditions correspond to the right-hand side column in Figure 5 top and down. The most straightforward difference can be found on product gas composition. Working under steam-oxygen gasification conditions results in a syngas product consisting mainly of CO_2 (ca. 60 vol.% content, dry N_2-free basis) due to the partial combustion of the SS for supplying the energy for the endothermic gasification reactions and the absence of CO_2 retention in the gasifier in this case. As indicated in Table 4, there were practically no $CaCO_3$ in the overflow solids collected in S-O2 test since the magnesite used as bed material consisted mainly of MgO (see composition in Table 3), which did not perform any CO_2 retention at the conditions used in the gasifier. Moreover, the H_2 content resulted in ca. 26 % (dry N_2-free basis), which is significantly lower than the H_2 content reached under SEG conditions (above 70 vol.% in all the cases). Light hydrocarbons content resulted also in lower values than under SEG conditions due to the promotion of oxidation reactions as well as the enhancement of cracking/reforming reactions due to the operation at high temperatures. The decomposition of these light hydrocarbons together with the higher fixed carbon conversion reached due to the operation at a higher temperature made the total product gas yield to be raised, reaching a value of 0.55 Nm^3 (dry N_2-free)/kg as seen in Figure 5 top. These differences in syngas yield and composition between SEG and steam/O_2

conditions translated into differences in cold gas efficiency (CGE) values. Concretely, CGE values calculated for the experiments summarised in Table 4 resulted in values ranging between 35 % and 50 % for SEG conditions and a significantly lower value for steam/oxygen gasification test (i.e. 27 %). Calculated values for SEG conditions in this work were lower than those found in the literature for large-scale SEG calculations, which range between 63 and 75% [42,43], due to the lower biomass conversion reached in this work that led to a lower gas yield production. Comparing the gasification conditions used, lower CGE resulted for steam/O_2 conditions than for SEG since the quality of the syngas produced (i.e. low H_2 content and significantly high CO_2 content) impacted severely on the LHV of the syngas produced (6.5 MJ/Nm^3), and thus on the calculated CGE.

3.2. Product gas impurities

As described previously in section 2.3.1, two different methods were used for the quantification of tar, namely gravimetric tar and GC-MS tar. The nature of the identified compounds in each type of tar is different. GC-MS tar consists of the most volatile tar compounds (i.e. benzene, toluene, xylene and naphthalene mainly), whereas gravimetric tar consists of naphthalene and heavier hydrocarbons that are present in a higher concentration due to the evaporation procedure followed for gravimetric tar determination (see section 2.3.1). Figure 6 top shows the gravimetric tar and GC-MS tar contents calculated for the experiments performed in this work. All contents have been expressed as tar mass per volume of dry gas. As appreciated in the figure, gravimetric tar contents were lower than GC-MS tar contents in the experiments performed in this work regardless of the gasifying agent and/or operating conditions used and contrarily to the trend observed in the literature for the gasification of SS [24,25]. The main reason

behind this behaviour is the use of CaO and magnesite as bed materials in this work, which are well-known natural catalysts for tar cracking and so favour the decomposition of heavier hydrocarbons [33]. Low gravimetric tar contents were found for the operating conditions shown in Table 4, which moved between 5 and 12 g/Nm^3 (dry gas) under SEG conditions and fall down to ca. 2 g/Nm^3 under steam-oxygen gasification conditions. As a matter of comparison, when using an inert solid bed like silica sand, gravimetric tar content reported in the literature for steam gasification of SS at 800 ºC and an S/C ratio of 1.5 was ca. 100 g/Nm^3 (dry gas), whereas the addition of 20 wt% of CaO in the solid bed made the tar content to decrease by ten times [25]. Alternatively, significantly lower gravimetric tar contents of 6 g/Nm^3 (dry gas) have been reported for steam-oxygen gasification using CaO as bed material and SS as fuel [22]. These results confirm that the catalytic effect of CaO and magnesite when being used as bed materials in this work is the reason behind the low gravimetric tar contents found, as well as the introduction of oxygen as gasifying agent for the S-O2 experiment.

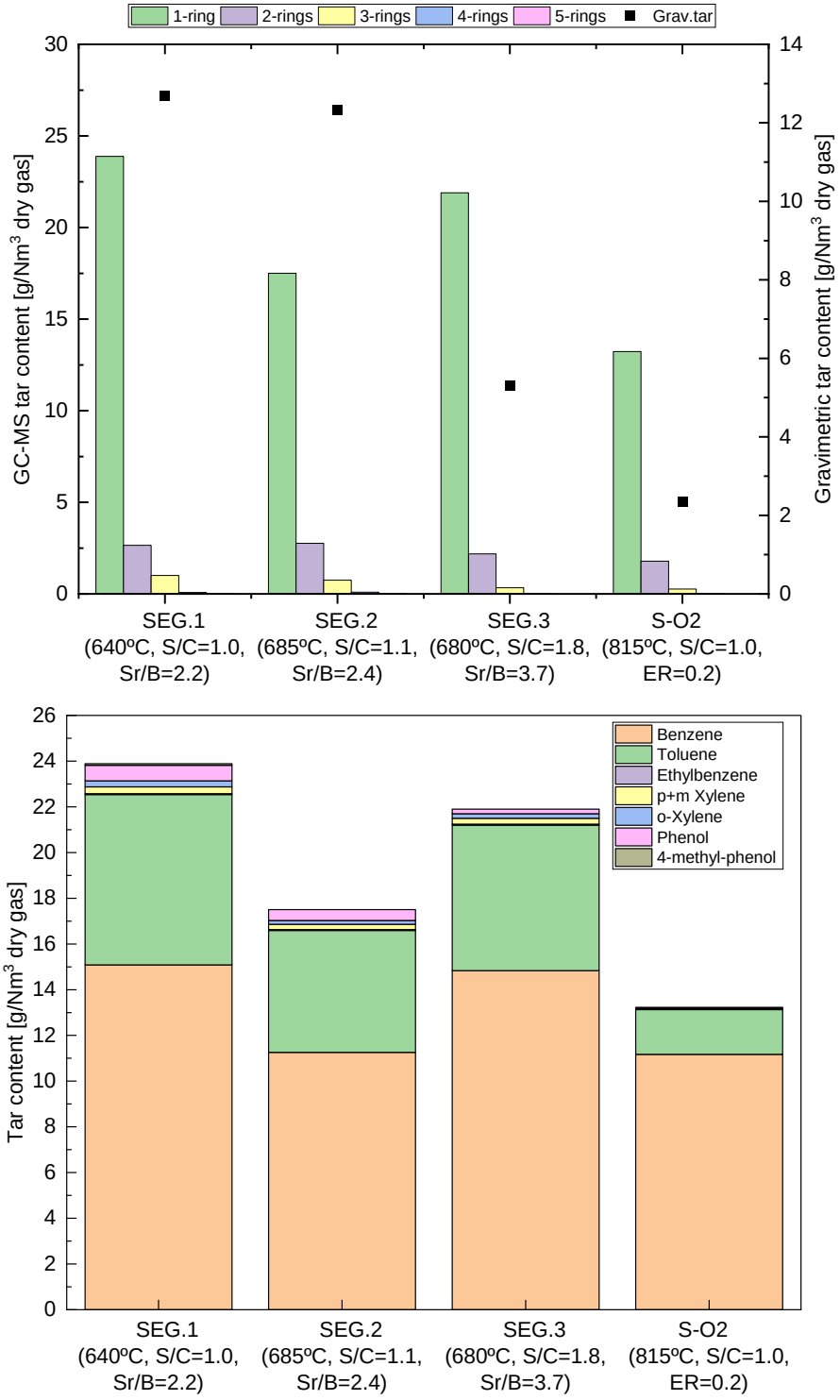

Figure 6. Tar content measurements (top) and 1-ring compounds content (down) for the experiments indicated in Table 4

Concerning the influence of operating parameters (temperature, S/C and Sr/B ratios) under SEG conditions, it can be noticed in Figure 6 top that GC-MS tar content was

influenced to a greater extent by the gasification temperature rather than by the S/C and Sr/B ratios used, whereas the gravimetric tar content barely changed with the temperature but changed appreciably with the Sr/B and S/C proportions. Main fluctuations in the GC-MS tar are due to the variations in the content of 1-ring compounds, which has been broken down into the individual compounds considered in Figure 6 down. As observed, benzene is the major 1-ring compound quantified and its variation with the temperature, the S/C and Sr/B proportions is reflected in the fluctuations observed in the GC-MS tar content. Naphthalene was the only 2-ring compound detected in this case whereas acenaphthylene, fluorene and phenanthrene were the main 3-ring compounds. These compounds were present in all the experiments performed in this work and barely changed when the operating conditions were modified. As already found in a previous work, working with high Sr/B ratios almost abated completely the formation of 4-6 rings compounds as can be noticed in Figure 6 top, which are the most dangerous aromatic hydrocarbons for human health [33]. Although it cannot be appreciated in the figure, the content of 4-6 rings compounds in experiments SEG.1 and SEG.2 was 0.08 and 0.11 g/Nm^3 (dry gas), respectively, and it decreased to 0.03 g/Nm^3 (dry gas) in experiment SEG.3 that corresponds to an increased Sr/B proportion of 3.8 (see detailed conditions in Table 4). The formation of these compounds was also almost abated under steam-oxygen gasification conditions (i.e. a content of 0.01 g/Nm^3 (dry gas) was calculated in this case) probably due to the operation at a high temperature in the presence of oxygen.

Other impurities detected in the syngas product corresponded to sulphur compounds, i.e. H_2S and COS. Table 6 shows the contents of H_2S and COS measured in the different experiments summarized in Table 4, and have been expressed in parts per million in the dry gas. The most straightforward effect that can be observed from the results in Table 6

is that the use of CaO as bed material in SEG experiments allows reducing noticeably H_2S emissions while COS is not detected in the syngas. The formation of CaS through reaction (eq. 1) as well as the enhanced conversion of COS into H_2S due to the larger content of H_2 in the syngas (eq. 2) should be the reasons behind these facts under SEG conditions.

$$H_2S + CaO \leftrightarrow CaS + H_2O \qquad \text{(Eq. 1)}$$

$$COS + H_2 \leftrightarrow H_2S + CO \qquad \text{(Eq. 2)}$$

Moreover, an increment in the gasification temperature and in the Sr/B proportion used in the gasifier made the H_2S content in the syngas to be reduced. Concretely, increasing gasification temperature from 640 ºC until 685 ºC resulted in a decrease of the H_2S content in the syngas from 831 ppm to 313 ppm (both dry basis), whereas increasing the Sr/B proportion in SEG.3 up to 3.7 made the H_2S content to be reduced to 215 ppm (dry basis). On the contrary, working under steam-oxygen gasification conditions made both H_2S and COS to be detected in the syngas, reaching noticeably higher contents of 1050 and 18 ppm (dry gas) respectively.

Table 6. Content of H_2S, COS and NH_3 in the syngas product (dry basis) obtained in the experiments summarized in Table 4

	H_2S (ppm, dry gas)	**COS (ppm, dry gas)**	**NH_3 (g/Nm^3 dry gas)**	**NH_3 (g/kg SS)**
SEG.1	831.1	0	47.0	15.0
SEG.2	313.0	0	52.2	25.6
SEG.3	214.7	0	36.9	13.7
S-O2	1050.3	18.0	17.6	9.7

Finally, NH_3 measurements in the syngas were performed in the experiments summarized in Table 4, obtaining the results indicated in Table 6. As noticed, NH_3 content in the syngas was noticeably high under SEG conditions, ranging from

37 g_{NH3}/Nm^3 (dry gas) to 52 g_{NH3}/Nm^3 (dry gas) that correspond to 0.05 and 0.07 m^3/m^3 (dry gas), respectively. The high contents of NH_3 measured can be explained by the high nitrogen content in the SS used as fuel in this work (see Table 1). According to the nitrogen balance solved in the gasifier, such NH_3 emissions correspond to a conversion rate of fuel nitrogen to NH_3 of 47 % and 66 %, respectively. Figure 7 shows the nitrogen balance for the SEG experiment with the highest NH_3 emissions (i.e. SEG.2 in Table 4) and for the steam-oxygen gasification experiment. As noticed in the figure for SEG conditions, the majority of the nitrogen introduced with the SS is converted into NH_3 in the gasifier, with a reasonable fraction of this nitrogen being released as N_2 in the syngas. Concretely, for experiment SEG.2, more than 93 % of the fuel nitrogen was released in the gasifier as NH_3 and N_2, remaining 6.8 % of the fuel nitrogen in the unconverted char that would be used as fuel in a secondary combustion in a dual fluidized bed SEG process and so be ultimately released as NO_X or N_2 in this reactor. For the rest of SEG experiments performed in this work, the fuel nitrogen in the unconverted char was also around 5-6 %. This nitrogen distribution among solid and gas products is typical of steam gasification in dual fluidized bed reactors [25,44], although the specific nitrogen distribution in gas products (i.e. between NH_3 and N_2) would be determined by operating parameters and reactor configuration.

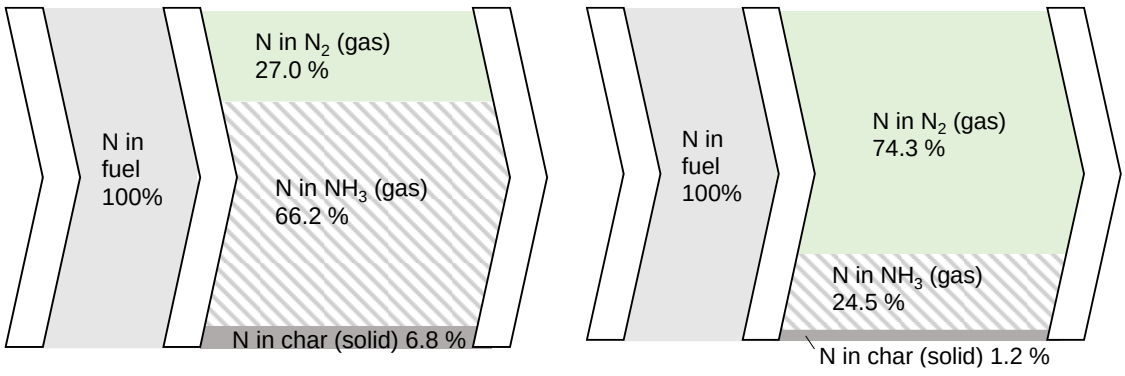

Figure 7. Nitrogen distribution in experiment SEG.2 (left) and S-O2 (right)

575 Regarding the influence of the gasification temperature, S/C and Sr/B proportions under
576 SEG conditions, the only clear effect that can be appreciated from the results in Table 6
577 is related to the Sr/B proportion. The increase in the Sr/B proportion made the NH_3
578 content in the syngas to be reduced from 52 to 37 g_{NH3}/Nm^3 (dry gas) while keeping the
579 gasification temperature at ca. 680-685 ºC, thanks to the addition of CaO that promotes
580 the reduction of NH_3 into N_2 probably due to its catalytic effect [25]. Finally, it has to
581 be noted that steam-oxygen gasification conditions clearly favour the reduction of the
582 NH_3 content in the syngas product with respect to steam gasification under SEG
583 conditions, as corroborated by other authors in the literature [24,25]. In this work, NH_3
584 concentration of ca. 18 g_{NH3}/Nm^3 (dry gas) (0.02 m^3/m^3(dry gas)) was measured for the
585 steam-oxygen gasification experiment.

586 **Conclusions**

587 The applicability of solar dried sewage sludge (SS) as feedstock material for a SEG
588 process has been satisfactorily demonstrated in a 30 kW_{th} bubbling fluidised-bed (BFB)
589 gasification pilot plant. The effect of the solid bed temperature, steam-to-carbon ratio,
590 sorbent-to-biomass ratio and gasification mode in product gas yield and composition, as
591 well as in the content of impurities has been assessed. Gasification temperature as well
592 as the gasification mode turned out to be the variables influencing the most the gas yield
593 and fixed carbon conversion obtained. Steam-oxygen gasification, while yielding the
594 highest gas yield (0.55 Nm^3(dry N_2-free)/kg) and fixed carbon conversion (89 %),
595 produced syngas of lower quality, mainly composed of CO_2 (60 vol%, dry N_2-free
596 basis), limiting its application for hydrogen or alternative synthetic fuel production. In
597 contrast, SEG conditions consistently produced syngas with high H_2 contents up to
598 70 vol% (dry N_2-free basis), nearly three times higher than in steam-oxygen

599 gasification. This substantial increase was attributed primarily to the use of CaO as the
600 bed material in SEG experiments. Additionally, the adoption of SEG conditions resulted
601 in a significant reduction in H_2S emissions, with no COS formation observed. By
602 further raising the gasification temperature and adjusting the Sr/B ratio, the H_2S content
603 in the syngas could be reduced to approximately 215 ppm (dry basis). Regarding N fate
604 in the gasifier, operating under SEG conditions made 93-95 % of the nitrogen
605 introduced with the SS to be obtained as NH_3 (mainly) and N_2 in the gasifier, with the
606 remaining nitrogen being recovered in the unconverted char. In comparison, steam-
607 oxygen gasification favoured the reduction of the NH_3 content in the syngas, with over
608 74 % of the nitrogen from SS being converted to N_2, what would simplify downstream
609 cleaning but would limit the use of the syngas produced for synthetic fuels production.
610 Finally, regarding tar content, gravimetric tar measurements consistently indicated
611 lower levels than those obtained through GC-MS analysis, regardless of the gasifying
612 agent and/or operating conditions due to the use of natural tar cracking catalysts (CaO
613 and magnesite) as bed materials. It was observed that GC-MS tar content was primarily
614 influenced by gasification temperature, whereas gravimetric tar content was more
615 responsive to variations in Sr/B and S/C ratios.

616 **Acknowledgements**

617 This work was partially funded by the project CSIC Biorrefinería TRE2021-03-011.
618 Samuel Moles thanks the grant Margarita Salas funded by the European Union-
619 NextGenerationEU. Isabel Martínez thanks the grant RYC2019-026929-I funded by
620 MCIN/AEI/10.13039/501100011033 and EI ‘‘ESF Investing in your future.” Authors
621 thank also the Regional Government of Aragón under the Research Groups Support
622 Program.

623

References

[1] Gozzo S, Moles S, Kińska K, Ormad MP, Mosteo R, Gómez J, et al. Screening for Antibiotics and Their Degradation Products in Surface and Wastewaters of the POCTEFA Territory by Solid-Phase Extraction-UPLC-Electrospray MS/MS. Water (Switzerland) 2023;15. https://doi.org/10.3390/w15010014.

[2] Kinuthia GK, Ngure V, Beti D, Lugalia R, Wangila A, Kamau L. Levels of heavy metals in wastewater and soil samples from open drainage channels in Nairobi, Kenya: community health implication. Sci Rep 2020;10:1–13. https://doi.org/10.1038/s41598-020-65359-5.

[3] Moles S, Gozzo S, Ormad MP, Mosteo R, Gómez J, Laborda F, et al. Long-Term Study of Antibiotic Presence in Ebro River Basin (Spain): Identification of the Emission Sources. Water 2022;14:1033. https://doi.org/10.3390/w14071033.

[4] Rodriguez-Mozaz S, Vaz-Moreira I, Varela Della Giustina S, Llorca M, Barceló D, Schubert S, et al. Antibiotic residues in final effluents of European wastewater treatment plants and their impact on the aquatic environment. Environ Int 2020;140:105733. https://doi.org/10.1016/j.envint.2020.105733.

[5] Moles S, Mosteo R, Gómez J, Szpunar J, Gozzo S, Castillo JR, et al. Towards the removal of antibiotics detected in wastewaters in the POCTEFA territory: Occurrence and TiO2 photocatalytic pilot-scale plant performance. Water (Switzerland) 2020;12:1–26. https://doi.org/10.3390/w12051453.

[6] Ghorbani M, Konvalina P, Walkiewicz A, Neugschwandtner RW, Kopecký M, Zamanian K, et al. Feasibility of Biochar Derived from Sewage Sludge to Promote Sustainable Agriculture and Mitigate GHG Emissions—A Review. Int J Environ Res Public Health 2022;19. https://doi.org/10.3390/ijerph191912983.

[7] EurEau. Europe's Water in Figures: An Overview of the European Drinking water and Waste Water Sectors. Brussels, Belgium.: 2021.

[8] Para M, Transici LA, Demogr ELR. Ministerio Para La Transición Ecológica Y El Reto Demográfico Secretaría De Estado De Medio Ambiente Direccion General Calidad Y Evaluación Ambiental Memoria Anual De Generación Y Gestión De Residuos Residuos De Competencia Municipal. 2020 2020.

[9] Geng H, Xu Y, Zheng L, Gong H, Dai L, Dai X. An overview of removing heavy metals from sewage sludge: Achievements and perspectives. Environ Pollut 2020;266:115375. https://doi.org/10.1016/j.envpol.2020.115375.

[10] Chan A, Salsali H, McBean E. Heavy metal removal (copper and zinc) in secondary effluent from wastewater treatment plants by microalgae. ACS Sustain Chem Eng 2014;2:130–7. https://doi.org/10.1021/sc400289z.

[11] Bennamoun L. Solar drying of wastewater sludge: A review. Renew Sustain Energy Rev 2012;16:1061–73. https://doi.org/10.1016/j.rser.2011.10.005.

[12] MAGRAMA. Orden AAA/1072/2013, de 7 de junio, sobre utilización de lodos de depuración en el sector agrario. Boletín Of Del Estado 2013:44966–73.

[13] European Commission. Directive (EU) 2018/851 of the European Parliament and of the Council of 30 May 2018 amending Directive 2008/98/EC on waste. Off J Eur Union 2018:(L-150/109-140).

[14] Egle L, Rechberger H, Krampe J, Zessner M. Phosphorus recovery from municipal wastewater: An integrated comparative technological, environmental and economic assessment of P recovery technologies. Sci Total Environ 2016;571:522–42. https://doi.org/10.1016/j.scitotenv.2016.07.019.

671 [15] Cheng WN, Yi H, Yu CF, Wong HF, Wang G, Kwon EE, et al. Biorefining
672 waste sludge from water and sewage treatment plants into eco-construction
673 material. Front Energy Res 2019;7:1–9.
674 https://doi.org/10.3389/fenrg.2019.00022.

675 [16] Świerczek L, Cieślik BM, Konieczka P. The potential of raw sewage sludge in
676 construction industry – A review. J Clean Prod 2018;200:342–56.
677 https://doi.org/10.1016/j.jclepro.2018.07.188.

678 [17] Yamuna Rani M, Bhagawan D, Himabindu V, Venkateswara Reddy V, Saritha P.
679 Preparation and characterization of green bricks using pharmaceutical industrial
680 wastes. Environ Sci Pollut Res 2016;23:9323–33.
681 https://doi.org/10.1007/s11356-015-5191-2.

682 [18] Syed-Hassan SSA, Wang Y, Hu S, Su S, Xiang J. Thermochemical processing of
683 sewage sludge to energy and fuel: Fundamentals, challenges and considerations.
684 Renew Sustain Energy Rev 2017;80:888–913.
685 https://doi.org/10.1016/j.rser.2017.05.262.

686 [19] Liang Y, Xu D, Feng P, Hao B, Guo Y, Wang S. Municipal sewage sludge
687 incineration and its air pollution control. J Clean Prod 2021;295:126456.
688 https://doi.org/10.1016/j.jclepro.2021.126456.

689 [20] Viswanathan K, Abbas S, Wu W. Syngas analysis by hybrid modeling of sewage
690 sludge gasification in downdraft reactor: Validation and optimization. Waste
691 Manag 2022;144:132–43. https://doi.org/10.1016/j.wasman.2022.03.018.

692 [21] Judex JW, Gaiffi M, Burgbacher HC. Gasification of dried sewage sludge: Status
693 of the demonstration and the pilot plant. Waste Manag 2012;32:719–23.
694 https://doi.org/10.1016/j.wasman.2011.12.023.

[22] Schmid M, Beirow M, Schweitzer D, Waizmann G, Spörl R, Scheffknecht G. Product gas composition for steam-oxygen fluidized bed gasification of dried sewage sludge, straw pellets and wood pellets and the influence of limestone as bed material. Biomass and Bioenergy 2018;117:71–7. https://doi.org/10.1016/j.biombioe.2018.07.011.

[23] Fuchs J, Schmid JC, Müller S, Hofbauer H. Dual fluidized bed gasification of biomass with selective carbon dioxide removal and limestone as bed material: A review. Renew Sustain Energy Rev 2019;107:212–31. https://doi.org/10.1016/j.rser.2019.03.013.

[24] Schmid M, Hafner S, Scheffknecht G. Experimental parameter study on synthesis gas production by steam-oxygen fluidized bed gasification of sewage sludge. Appl Sci 2021;11:1–27. https://doi.org/10.3390/app11020579.

[25] Schweitzer D, Gredinger A, Schmid M, Waizmann G, Beirow M, Spörl R, et al. Steam gasification of wood pellets, sewage sludge and manure: Gasification performance and concentration of impurities. Biomass and Bioenergy 2018;111:308–19. https://doi.org/10.1016/j.biombioe.2017.02.002.

[26] Schmid M, Hafner S, Biollaz S, Schneebeli J, Waizmann G, Scheffknecht G. Steam-oxygen gasification of sewage sludge: Reduction of tar, H2S and COS with limestone as bed additive. Biomass and Bioenergy 2021;150. https://doi.org/10.1016/j.biombioe.2021.106100.

[27] Beheshti SM, Ghassemi H, Shahsavan-Markadeh R. Process simulation of biomass gasification in a bubbling fluidized bed reactor. Energy Convers Manag 2015;94:345–52. https://doi.org/10.1016/j.enconman.2015.01.060.

[28] Khanlari A, Doğuş Tuncer A, Sözen A, Şirin C, Gungor A. Energetic,

719 environmental and economic analysis of drying municipal sewage sludge with a
720 modified sustainable solar drying system. Sol Energy 2020;208:787–99.
721 https://doi.org/10.1016/j.solener.2020.08.039.

722 [29] Singh V, Phuleria HC, Chandel MK. Estimation of energy recovery potential of
723 sewage sludge in India: Waste to watt approach. J Clean Prod 2020;276:122538.
724 https://doi.org/10.1016/j.jclepro.2020.122538.

725 [30] Magdziarz A, Wilk M. Thermal characteristics of the combustion process of
726 biomass and sewage sludge. J Therm Anal Calorim 2013;114:519–29.
727 https://doi.org/10.1007/s10973-012-2933-y.

728 [31] Jayaraman K, Gökalp I. Pyrolysis, combustion and gasification characteristics of
729 miscanthus and sewage sludge. Energy Convers Manag 2015;89:83–91.
730 https://doi.org/10.1016/j.enconman.2014.09.058.

731 [32] Martínez I, Kulakova V, Grasa G, Murillo R. Experimental investigation on
732 sorption enhanced gasification (SEG) of biomass in a fluidized bed reactor for
733 producing a tailored syngas. Fuel 2020;259:116252.
734 https://doi.org/10.1016/j.fuel.2019.116252.

735 [33] Martínez I, Grasa G, Callén MS, López JM, Murillo R. Optimised production of
736 tailored syngas from municipal solid waste (MSW) by sorption-enhanced
737 gasification. Chem Eng J 2020;401:126067.
738 https://doi.org/10.1016/j.cej.2020.126067.

739 [34] Martínez I, Callén MS, Grasa G, López JM, Murillo R. Sorption-enhanced
740 gasification (SEG) of agroforestry residues: Influence of feedstock and main
741 operating variables on product gas quality. Fuel Process Technol 2022;226:0–10.
742 https://doi.org/10.1016/j.fuproc.2021.107074.

[35] Chen YH, Parvez AM, Schmid M, Scheffknecht G, Chen TL. 20 kW Pilot scale steam-oxygen gasification of solid recovered fuel with a focus on newly developed off-line and on-line tar measurement methods. Fuel Process Technol 2022;227:107096. https://doi.org/10.1016/j.fuproc.2021.107096.

[36] Pecate S, Kessas SA, Morin M, Hemati M. Beech wood gasification in a dense and fast internally circulating fluidized bed. Fuel 2019;236:554–73. https://doi.org/10.1016/j.fuel.2018.09.025.

[37] Aznar MP, Gracia-Gorria FA, Corella J. Minimum and maximum velocities for fluidization for mixtures of agricultural and forest residues with a second fluidized solid. I. Preliminary data and results with sand-sawdust mixtures. Int Chem Eng 1992;32:95–102.

[38] Neeft JPA. Rationale for setup of impinger train as used in the technical specification of sampling and analysis of tar and particles in the product gases of biomass gasification. Tech Backgr Doc CEN BT/TF 2005:1–14.

[39] US Environmental Protection Agency (EPA). Method 17: determination of particulate matter emissions from stationary sources 2017:1–7.

[40] Florin NH, Harris AT. Enhanced hydrogen production from biomass with in situ carbon dioxide capture using calcium oxide sorbents. Chem Eng Sci 2008;63:287–316. https://doi.org/10.1016/j.ces.2007.09.011.

[41] Tilman J. Schildhauer (Editor) SMAB (Editor). Synthetic Natural Gas from Coal, Dry Biomass, and power-to-gas applications. Wiley-Blackwell; 2016.

[42] Poluzzi A, Guandalini G, Guffanti S, Elsido C, Moioli S, Huttenhuis P, et al. Flexible Power & Biomass-to-Methanol plants: Design optimization and

766 economic viability of the electrolysis integration. Fuel 2022;310:122113.
767 https://doi.org/10.1016/j.fuel.2021.122113.

768 [43] Martínez I, Romano MC. Flexible sorption enhanced gasification (SEG) of
769 biomass for the production of synthetic natural gas (SNG) and liquid biofuels:
770 Process assessment of stand-alone and power-to-gas plant schemes for SNG
771 production. Energy 2016;113:615–30.
772 https://doi.org/10.1016/j.energy.2016.07.026.

773 [44] Wilk V, Hofbauer H. Conversion of fuel nitrogen in a dual fluidized bed steam
774 gasifier. Fuel 2013;106:793–801. https://doi.org/10.1016/j.fuel.2012.12.056.

775